RSC Advances




ROYAL SOCIETY OF CHEMISTRY

www.rsc.org/advances

Journal Name

RSCPublishing

ARTICLE

Cite this: DOI: 10.1039/x0xx00000x

Received 00th January 2012,
Accepted 00th January 2012

DOI: 10.1039/x0xx00000x

www.rsc.org/

# New Supramolecular Compounds Based on Porphyrin and Polyoxometalate: Synthesis, Characterization and Nonlinear Optical and Optical Limiting Properties

Zonghai Shi,[a] Yunshan Zhou,[*a,b] Lijuan Zhang,[*a] Cuncun Mu,[a] Haizhou Ren,[a] Daf ul Hassan,[a] Di Yang[a] and Hafiz Muhammad Asif[a]

Three new supramolecular compounds $[H_2TPP]_{1.5}[SW_{11}VO_{40}]\cdot 5CH_3CN\cdot 4H_2O$ **1**, $[H_2TPP]_2[SW_{10}V_2O_{40}]\cdot 4CH_3CN\cdot 3H_2O$ **2**, $[H_2TPP][SW_{12}O_{40}]\cdot 4H_2O$ **3** composed of $[H_2TPP]^{2+}$ cation and vanadium substituted Keggin-type polyoxometalate (POM) anion $[SW_{12-n}V_nO_{40}]^{(2+n)-}$ (n = 0 - 2) were prepared and characterized. The third-order nonlinear optical (NLO) and optical limiting (OL) properties of resulting hybrids were studied by using an Nd:YAG laser at 532 nm with a pulse duration of $\tau$ = 7 ns. The results demonstrate that all of these supramolecular compounds have significant nonlinear reverse saturated absorption, self-defocusing behavior, and good OL performance, especially for compound **1**, which has a second hyperpolarizability $\gamma$ value of $7.05 \times 10^{-29}$ (esu) and exhibits a comparable OL performance with the most well-known OL materials such as In(Pc*)Cl indicating that they are potentially excellent NLO materials. Remarkably, it was also observed that the degree of vanadium substitution in POM anions corresponding to different onset of reduction potential influences the NLO and OL properties of the resulting compounds: third-order NLO and OL properties of compound **2** is inferior to that of compound **1**, and is better than that of compound **3**. Both their second hyperpolarizability $\gamma$ values and the OL performance were observed inversely proportional to the HOMO-LUMO gaps of the resulting compounds. The excited charge transfer from porphyrin to POM anions in the supramolecular compounds when exposed in laser is thought to play key role in the enhancement of NLO and OL response.

## 1. Introduction

Materials with nonlinear optical properties and fast response to laser as well as with merits such as small optical loss, high optical quality, good stability, low cost and ease of preparation, have attracted increasing attention owing to their potential applications in ultrafast optical switching, optical communication, optical modulators and optical limiting.[1-5] In this context, a lot of studies, based on organic-[6], inorganic-[7], metal-organic-[8], organic low-molecular-[9], polymeric-[10], organic-inorganic hybrid- materials[11], *etc*., have been done. Among the NLO materials concerned, organic-inorganic hybrid materials have emerged as promising candidates due to integrating the virtues of both inorganic and organic materials, and been widely studied in the field of nonlinear optics in the past decade.[12-14]

Porphyrins are comprised of four pyrrole units linked together through their α-positions by methine bridges. The highly delocalized aromatic 18 π-electron system of porphyrins can give rise to a strong NLO response.[15] They have been extensively investigated as being among the most promising of NLO materials due to their architectural flexibility, which allows tailoring of their physical, optoelectronic and chemical parameters in a broad range, having exceptional stability and processability features.[16] The variety of methods were adopted to obtain the porphyrin-based material with excellent performance in NLO, wherein the grafting electron acceptor (such as multi-walled carbon nanotube, single-walled carbon nanotube, graphene, $C_{60}$, ferrocene, *etc*.) to porphyrin forming organic-inorganic hybrid were proved to be one of the effective methods.[17-21]

On the other hand, polyoxometalates (POMs), a class of metal–oxygen cluster compound having remarkable structural diversity and chemical composition variety, have shown unique physicochemical properties and are used in various applications.[22,23] In particular, POM anions are a kind of good electron acceptor and have the ability to undergo photoexcitation to perform electron transfers from LMCT by

trapping photogenerated electrons.[24] Therefore, the combination of POMs and porphyrin forming porphyrin-POM supramolecular compounds may facilitate photogenerated electron transfer and further improve the NLO properties of porphyrin. So far, three theoretical studies are reported about the second-order NLO properties of the porphyrin-POM systems where the systems are found to possess remarkably large static second-order polarizabilities due to charge transfer between porphyrin and POMs.[25-27] These studies demonstrate that the integration between Porphyrins and POMs are expected to produce new type of excellent NLO materials. We have recently reported third-order NLO properties of a type of hybrids[28] composed of the keggin-type POM anions possessing different central heteroatoms and coordination atoms, namely, $PMo_{12}O_{40}^{3-}$, $SiM_{12}O_{40}^{4-}$ (M = W, Mo) and $PMo_{10}V_2O_{40}^{5-}$. While the research demonstrates that combination of POMs and porphyrins forming porphyrin-POM hybrids can significantly enhance third-order NLO susceptibility of porphyrins, a lot of work still needs to be done in order to have more deep insight in understanding inherent property-structure relationship and the rational design of POM-porphyrin systems having excellent potential as NLO materials.

Following our continuous efforts investigating NLO materials and their consequent practical applications[29-36], we are especially interested in investigation on effect of heteroatom substitution in POM anions on the third-order NLO and OL properties of the resulting system. In this work, the Keggin-type POM anions, with same central heteroatom and coordination atom, but different degree of vanadium substitution, $[SW_{12-n}V_nO_{40}]^{(2+n)-}$ (n = 0 - 2) (Fig. 1), were selected as a protype, and three supramolecular compounds $[H_2TPP]_{1.5}[SW_{11}VO_{40}]\cdot 5CH_3CN\cdot 4H_2O$ **1**, $[H_2TPP]_2[SW_{10}V_2O_{40}]\cdot 4CH_3CN\cdot 3H_2O$ **2**, $[H_2TPP][SW_{12}O_{40}]\cdot 4H_2O$ **3** composed of $[H_2TPP]^{2+}$ cation (Fig. 1) and $[SW_{12-n}V_nO_{40}]^{(2+n)-}$ (n = 0 - 2) anion were prepared and characterized. While all of the resulting compounds showed significant nonlinear reverse saturated absorption, self-defocusing behavior, and good OL performance, vanadium substitution in POM anions corresponding to different onset of reduction potential was observed to influence the NLO and OL properties of the resulting compounds.

## 2. Experimental

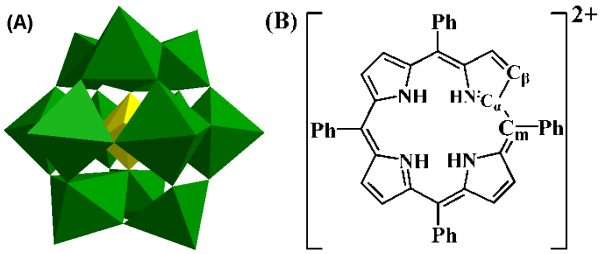


Fig. 1 The vanadium-substituted Keggin-type POM anions $[SW_{12-n}V_nO_{40}]^{(2+n)-}$ (n = 0 - 2) in polyhedral representation (A) (color code: W/$VO_6$ octahedra, green; $SO_4$ tetrahedron, yellow) and divalent cations of porphyrin $[H_2TPP]^{2+}$ (B) used in this study.

### 2.1 Instruments and Material

IR spectra were recorded on a Nicolet 6700 spectrophotometer with KBr pellet in the range of 400-4000 $cm^{-1}$. The UV-vis. spectra were recorded with a Shimadzu UV-2550 spectrophotometer in the range of 200-800 nm. Thermogravimetric analyses were carried out on a TGAQ50 instrument at a heating rate of 10 °C/min under air atmosphere. Elemental analyses for C, H and N were performed on Perkin-Elmer 240C analytical instrument. ICP analyses for S, W and V were determined by ULTIMA type analytical instrument. Cyclic voltammograms (CV) were obtained on a CHI660B electrochemical analyzer in dry DMF at room temperature at the rate of 10 mV/s in the presence of 0.1 M $[(n\text{-butyl})_4N]PF_6$ as a supporting electrolyte. A glassy carbon electrode was used as a working electrode, Ag/AgCl as a reference electrode and a Pt wire as an auxiliary electrode. The scan range of the CV were selected carefully from the wide range (+2.5 V ~ - 2.5 V) to small range (present in the paper) to insure the peak used for calculating the HOMO or LUMO levels is the onset peaks. NLO properties were performed by using an EKSPLA NL303 Q-switched Nd:YAG laser at 532 nm with a pulse duration of τ = 7 ns, a repetition rate of 10 Hz and the intensity of the light at focus $E_0$ being 6.4 uJ. The laser beams were focused into the sample placed in a quartz cell with a 1-mm-path-length spectroscopic cell, the waist $\omega_0$ was measured to be 19 μm. The linear transmittance of the far-field aperture *S* was measured to be 0.25. The value of $n_0$ was measured to be *ca*. 1.429 for all the samples. The samples were proved to be stable towards air and laser light under the experimental conditions. Before the measurements, the system was calibrated using $CS_2$ as reference. OL performances of all the samples in DMF were tested by using an EKSPLA NL303 Q-switched Nd:YAG laser. Tetraphenylporphyrin (TPP),[37] $(n\text{-}Bu_4N)_3[SVW_{11}O_{40}]$ ($SWV_1$), $(n\text{-}Bu_4N)_4[SV_2W_{10}O_{40}]$ ($SWV_2$), and $(n\text{-}Bu_4N)_2[SW_{12}O_{40}]$ (SW)[38] were prepared according to the literature methods. All the other chemicals were purchased from Aladdin Industrial Inc., were of analytical grade and used without further purification. Solvents were used as received or dried using standard procedures.

### 2.2 Preparation of compounds $[H_2TPP][ClO_4]_2$ and 1 – 3

**$[H_2TPP][ClO_4]_2$**: TPP (180 mg) was dissolved in 20 mL tetrahydrofuran (THF). The green solid powder appeared simultaneously after 6 mL of concentrated perchloric acid was added. The product was collected by vacuum filtration and washed with water and THF, respectively, and air-dried (200.2 mg, 85% based on TPP). Anal. Calcd for $C_{44}H_{32}N_4Cl_2O_8$: C, 64.65; N, 6.86; H, 3.92%. Found: C, 64.38; N, 6.98; H, 4.13%.

**$[H_2TPP]_{1.5}[SW_{11}VO_{40}]\cdot 5CH_3CN\cdot 4H_2O$ 1**: $[H_2TPP][ClO_4]_2$ (67.5 μmol, 54.9 mg) and $SWV_1$ (30 μmol, 104 mg) were dissolved in 17 mL of $CHCl_3$ and 10 mL of $CH_3CN$, respectively. The green solid powder appeared simultaneously after mixed the two solutions with stirring. The product was collected by vacuum filtration and washed with $CHCl_3$ and

$CH_3CN$, respectively, and air-dried (106.8 mg, 70% based on $SWV_1$). Anal. Calcd for $C_{76}H_{71}N_{11}O_{44}SW_{11}V$: C, 23.72; H, 1.85; N, 4.00; S, 0.83; W, 52.59; V, 1.32 %. Found: C, 23.98; H, 1.82; N, 4.29, S, 0.71; W, 52.38; V, 1.28 %.

**$[H_2TPP]_2[SW_{10}V_2O_{40}]\cdot 4CH_3CN\cdot 3H_2O$ 2**: $[H_2TPP][ClO_4]_2$ (34 μmol, 27.6 mg) and $SWV_2$ (15 μmol, 53.8 mg) were dissolved in 15 mL of $CHCl_3$ and 7.5 mL of $CH_3CN$, respectively. The green solid powder appeared simultaneously after mixing the two solutions with stirring. The product was collected by vacuum filtration and washed with $CHCl_3$ and $CH_3CN$ respectively, and air-dried (55.6 mg, 65% based on $SWV_2$). Anal. Calcd for $C_{96}H_{82}N_{12}O_{43}SW_{10}V_2$: C, 28.35; H, 2.02; N, 4.13; S, 0.79; W, 45.24; V, 2.51 %. Found: C, 28.15; H, 2.07; N, 4.08; S, 0.93; W, 45.36; V, 2.29 %.

**$[H_2TPP][SW_{12}O_{40}]\cdot 4H_2O$ 3**: $[H_2TPP][ClO_4]_2$ (45 μmol, 36 mg) and SW (30 μmol, 100 mg) were dissolved in 15 mL of $CHCl_3$ and 10 mL of $CH_3COCH_3$, respectively. The green solid powder appeared simultaneously after the two solutions were mixed with stirring. The product was collected by vacuum filtration and washed with $CHCl_3$ and $CH_3COCH_3$, respectively, and air-dried (59.1 mg, 50% based on SW). Anal. Calcd for $C_{44}H_{40}N_4O_{44}SW_{12}$: C, 14.81; H, 1.12; N, 1.57; S, 0.90; W, 61.85 %. Found: C, 15.00; H, 1.08; N, 1.54; S, 0.72; W, 61.93 %.

## 3. Results and discussion

The IR spectra of $[H_2TPP][ClO_4]_2$, parent POMs ($SWV_1$, $SWV_2$, and SW) and compounds **1** - **3** are shown in Fig. S1. The observed major IR bands and their assignments along with mode number are listed in Table S1. All the N-H, C-H and C=C stretching vibration of benzene ring, as well as C=N stretching vibration of pyrrole ring, characteristic infrared bands in the 780 – 1190 $cm^{-1}$ region assigned to S-$O_a$, W=$O_t$, W-$O_c$-W and W-$O_b$-W stretching vibrations (Table S1)[38] are found in the IR spectra of compounds **1** - **3**, indicating that the structures of $[H_2TPP]^{2+}$ and POM anions remain intact in the resulting porphyrin–POM hybrids. The bands with lower intensities observed at 700 – 1600 $cm^{-1}$ and near 3300, 3100 $cm^{-1}$ further confirm the presence of the organic moieties $[H_2TPP]^{2+}$ in the porphyrin-POM hybrids (Fig. S1). Compared the IR spectra of the resulting supramolecular porphyrin-POM compounds with those of parent POMs, the vibrational bands of the S-$O_a$, W-$O_t$, W-$O_b$-W and W-$O_c$-W bond have a red-shift for all hybrids implying that these bonds are weakened to some extent due to the drastic interaction between the $[H_2TPP]^{2+}$ and POMs anions.

The electronic properties of the resulting compounds **1** - **3** in DMF are studied by UV-vis spectroscopy (Fig. S2). All the hybrid compounds have absorption peaks around 266, 416, 513, 547, 590 and 645 nm. The peak at 266 nm can be assigned to the tungsten-oxygen charge transfer absorption[38], the absorption peak around 416 nm can be attributed to the porphyrin Soret band, while the four typical weak absorptions peaks appearing at 513, 547, 590 and 645 nm are assigned to Q bands[39]. This further indicates that the porphyrin-POM hybrids have been successfully synthesized, and the structure of both

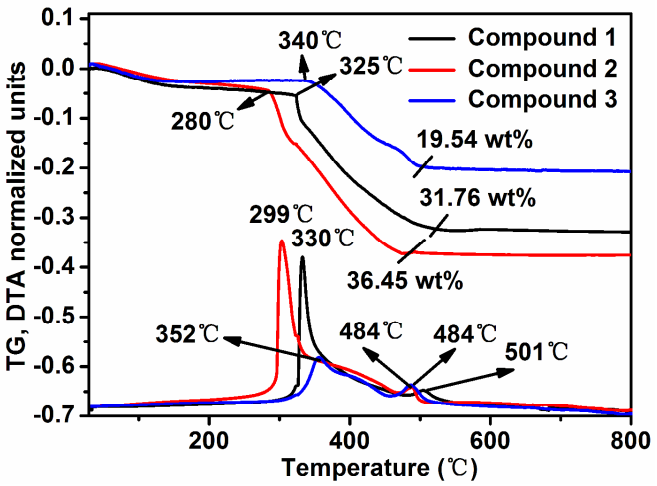


Fig. 2. TG curves of compounds **1** - **3**.

POMs anions and $[H_2TPP]^{2+}$ are maintained in the porphyrin-POM hybrids. Obviously, the absorption bands positions and intensity of the POMs and $[H_2TPP]^{2+}$ do not show significant changes as compared to the individual reactants, and no additional band is observed (Table S2). This result indicates the lack of strong electronic interaction in the ground state between the $[H_2TPP]^{2+}$ and POMs anion in the dilute solution.[40]

In order to investigate the thermostability and confirm the molecule formulas of compounds **1** - **3** given by elemental analyses, we performed thermogravimetric analyses. The TG curves of compounds **1** - **3** are shown in Fig. 2. Compounds **1** - **3** lose all of the organic part, lattice solvent and water molecules in one step. From 28 to 520 □, the weight loss of compound **1** is 31.76 % with two corresponding exothermal peaks at 330 and 501 °C in DTA curve, respectively, which is corresponded to loss of 4 lattice water, 5 lattice $CH_3CN$ and 1.5 TPP (calculated value: 31.27 %). Compound **2** loses 36.45 % in weight in the temperature range of 28 - 475 □, corresponding to loss of 2 TPP, 3 water and 4 $CH_3CN$ (calculated value: 35.99%) with two corresponding exothermal peaks at 299 and 484 °C in DTA curve, respectively. From 28 to 500 □, compound **3** loses 19.54 % in weight corresponding to loss of 1 TPP and 4 water (calculated value: 19.38 %) with two corresponding exothermal peaks at 352 and 484 □ in DTA curve, respectively. Thermogravimetric analyses of compounds **1** - **3** match well with the element analyses results. From Fig. 2, it is observed that the organic part $[H_2TPP]^{2+}$ of compounds **1** - **3** begins to decompose at 325, 280 and 340 □, respectively.[41] The thermostability of compounds **1** - **3** are decreasing in following order: **2** < **1** < **3**, which reflects the drastic interaction between the porphyrin cations and the POM anions in solid state. The more negative charges the POM anions $[SW_{12-n}V_nO_{40}]^{(2+n)-}$ (n = 0 - 2) have, the more drastic interaction between anions and cations in the hybrid compounds resulting lower decomposition temperature.

The stoichiometries of compounds **1** - **3** have also been investigated by the Job's plot analysis using the absorption

Journal Name RSCPublishing

ARTICLE

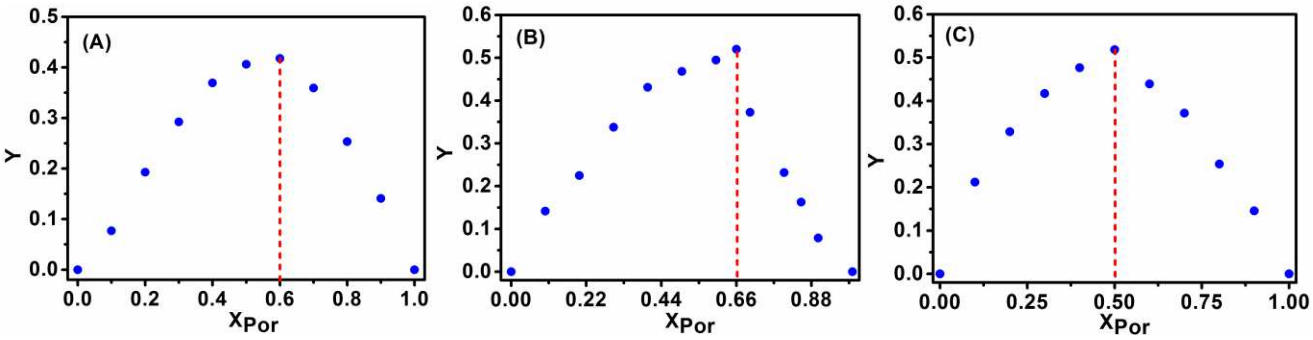


Fig. 3 the Job's plots analysis for $[H_2TPP]^{2+}$ and $[SVW_{11}O_{40}]^{3-}$ (A), $[SV_2W_{10}O_{40}]^{4-}$ (B) and $[SW_{12}O_{40}]^{2-}$ (C) (λ = 419 nm). The red dash lines show the maximum values of $X_{Por}$

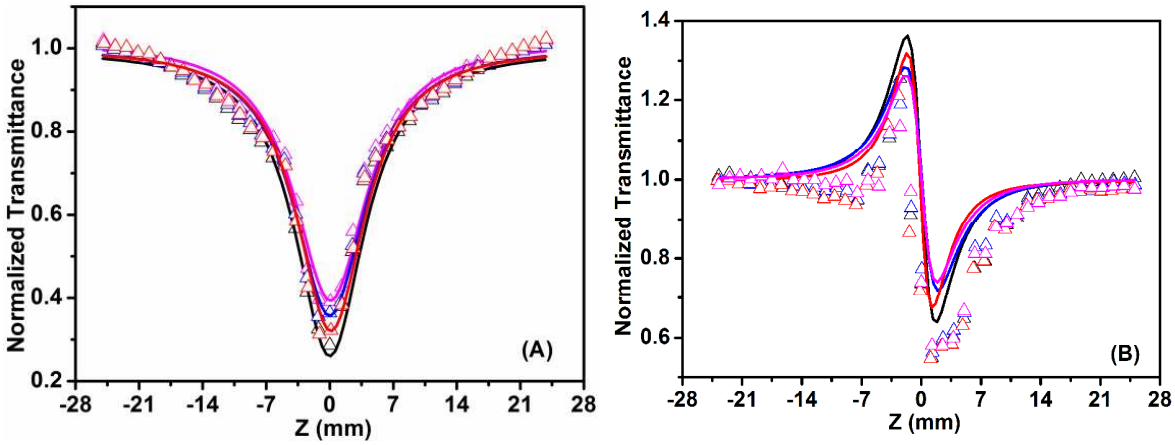


Fig. 4. Z-scan curves of compounds **1** - **3** and $[H_2TPP][ClO_4]_2$ in DMF (A: open-aperture curves; B: closed-aperture curves; black: compound **1** ($1.98 \times 10^{-4}$ mol·L$^{-1}$); red: compound **2** ($1.51 \times 10^{-4}$ mol·L$^{-1}$); green: compound **3** ($3.02 \times 10^{-4}$ mol·L$^{-1}$); pink: $[H_2TPP][ClO_4]_2$ ($2.92 \times 10^{-4}$ mol·L$^{-1}$); the open triangles indicate the measured data; the solid curves are theoretical fits). (Note: The concentrations deliberately selected herein can guarantee the linear transmittance of DMF solutions of compounds **1** – **3** and $[H_2TPP][ClO_4]_2$ being 0.7 at 532 nm).

changes at 419 nm (Fig. S3). The analytical solutions of varying porphyrin/POMs molar ratios were prepared by keeping the total molarity of porphyrin and POMs constant ($5 \times 10^{-6}$ mol·L$^{-1}$). In this context, the corrected absorbance, *Y*, is defined as:[42]

$$Y = A - Cb(\varepsilon_{Por} X_{Por} + \varepsilon_{POM} X_{POM}) \quad (1)$$

where *A* is the measured optical absorbance of the solution at 419 nm (Fig. S3), *C* = [porphyrin] + [POM] is the total concentration, b is the optical path length, $X_{Por}$ = [porphyrin]/C and $X_{POM}$ = [POM]/C is the mole fraction of porphyrin and POMs, $\varepsilon_{Por}$ ($2.9 \times 10^5$ L·mol$^{-1}$·cm$^{-1}$) and $\varepsilon_{POM}$ ($3.6 \times 10^2$, $5.1 \times 10^2$ and $2.5 \times 10^2$ L·mol$^{-1}$·cm$^{-1}$ for $SWV_1$, $SWV_2$ and SW, respectively) are the molar extinction coefficients of the porphyrin and POMs at 419 nm, respectively. Thus, *Y* represents a deviation of the absorbance of the solution from the additivity of absorbance for the porphyrin and the POMs.

The Job's plots were obtained by plotting *Y* against $X_{Por}$ (Fig. 3). The plots, with three maximums at a mole fraction of 0.6, 0.67, 0.5, confirm unequivocally the formation of the 1.5:1, 2:1, 1:1 complexes between $[H_2TPP]^{2+}$ and $[SVW_{11}O_{40}]^{3-}$, $[SV_2W_{10}O_{40}]^{4-}$ and $[SW_{12}O_{40}]^{2-}$ respectively, matching well with elemental analyses and TG results.[42]

The Z-scan curves along with corresponding fits for compounds **1** - **3** and $[H_2TPP][ClO_4]_2$ are shown in Fig. 4. Reasonably good matches between observed experimental data and theoretical curves are observed. The results suggest that the experimentally detected NLO effects have an effective third-order characteristic. All of the compounds have notable nonlinear reverse saturated absorption (RSA) under the open-aperture configuration corresponding to a positive nonlinear

absorption coefficient $\beta$ (Fig. 4A), a property that is widely applicable in the protection of optical sensors.[43] Each of theclosed-aperture Z-scan curves for compounds **1** - **3** and $[H_2TPP][ClO_4]_2$ have a peak-valley configuration corresponding to a negative nonlinear refractive index and a characteristic self-defocusing behavior of the propagating wave in the compounds (Fig. 4B). Since pristine DMF and parent POMs have negligible third-order NLO effect (Fig. S4) under the same experimental conditions, the porphyrin moieties are considered to be the only source for NLO properties of resulting porphyrin-POM hybrids.

The following formula are used to calculate the third-order nonlinear refractive index $n_2$ (esu), nonlinear absorption coefficient $\beta$ (esu) and optical nonlinear susceptibility $\chi^{(3)}$ (esu).[44]

$$\Delta T_{P-V} = 0.406(1-S)^{0.25}\left|\Delta\phi_0\right| \quad (2)$$

$$\Delta\phi_0 = kL_{eff}\gamma I_0 \quad (3)$$

$$L_{eff} = (1-e^{-\alpha_0 L})/\alpha_0 \quad (4)$$

$$n_2(esu) = \frac{cn_0}{40\pi}\gamma(m^2/W) \quad (5)$$

where, $\Delta T_{P-V}$ is the normalized peak-valley difference, $\Delta\varphi_0$ is the phase shift of the beam at the focus, $K = 2\pi/\lambda$ is the wave vector, $I_0$ (unit: W/m$^2$) is the intensity of the light at focus, $L_{eff}$ is the effective length of the sample defined in terms of the linear-absorption coefficient $\alpha_0$ and the true optical path length through the sample, $n_0$ is the linear refractive index, and $\gamma$ is optical Kerr constant. The conversion can be realized between $n_2$ (esu) and $\gamma$ (m$^2$/W) by eq (5).

When the sample is measured under open aperture, the normalized transmittance T (z, s = 1) can be expressed as

$$T(z, s=1) = \sum_{m=0}^{\infty}\frac{[-q_0(z)]^m}{(m+1)^{3/2}} \quad (6)$$

Where $q_0(z) = \dfrac{\beta I_0 L_{eff}}{(1+z^2/z_0^2)}$, $\beta$ is nonlinear absorption coefficient.

From eq (6) we can get $\beta$. From eq (7), we can get the third-order optical nonlinear susceptibility $\chi^{(3)}$.

$$\chi^{(3)} = \sqrt{\left(\frac{cn_0}{160\pi^2}\gamma\right)^2 + \left(\frac{c\beta n_0^3\lambda}{64\pi^3}\right)^2} \quad (7)$$

The molecular second hyperpolarizability $\gamma$ of the samples was calculated by following equation:[45]

$$\gamma = \frac{\chi^{(3)}}{N_C L} \quad (8)$$

Where $n_0$ is the linear refractive index of sample, $N_c$ is the molecular number density per cubic centimetre, and $L$ is the local-field correction factor, which may be approximated by $[(n_0^2+2)/3]^4$.[45]

Using eqs (5), (6), (7) and (8), the nonlinear refractive index $n_2$, nonlinear absorption coefficient $\beta$, third-order optical nonlinear susceptibility $\chi^{(3)}$ and second hyperpolarizability $\gamma$ (based on $[H_2TPP]^{2+}$) are calculated (Table 1). The data listed in Table 1 not only show that compounds **1** - **3** have large $\chi^{(3)}$ and second hyperpolarizability $\gamma$ values but also show that the $\gamma$ values of compounds **1** - **3** ($\gamma$ (**1**), $\gamma$ (**2**), $\gamma$ (**3**)) are improved when compared with that of $[H_2TPP][ClO_4]_2$. In addition, it is observed that third-order NLO properties of compound **2** having anion $[SW_{10}V_2O_{40}]^{4-}$ is inferior to that of compound **1** having anion $[SW_{11}VO_{40}]^{3-}$, better than that of compound **3** having anion $[SW_{12}O_{40}]^{2-}$. This observation clearly shows that the POMs with different degree of vanadium substitution impose remarkable effect on the third-order nonlinear optical properties of resulting porphyrin-POM hybrid systems.

The energy dependent transmission measurement results of compounds **1** - **3** and $[TPP][ClO_4]_2$ are shown in Fig. 5A. From Fig. 5A we can know that the transmission is significantly reduced respectively from 70% to 24.1%, 23.0%, 26.4%, 27.2%

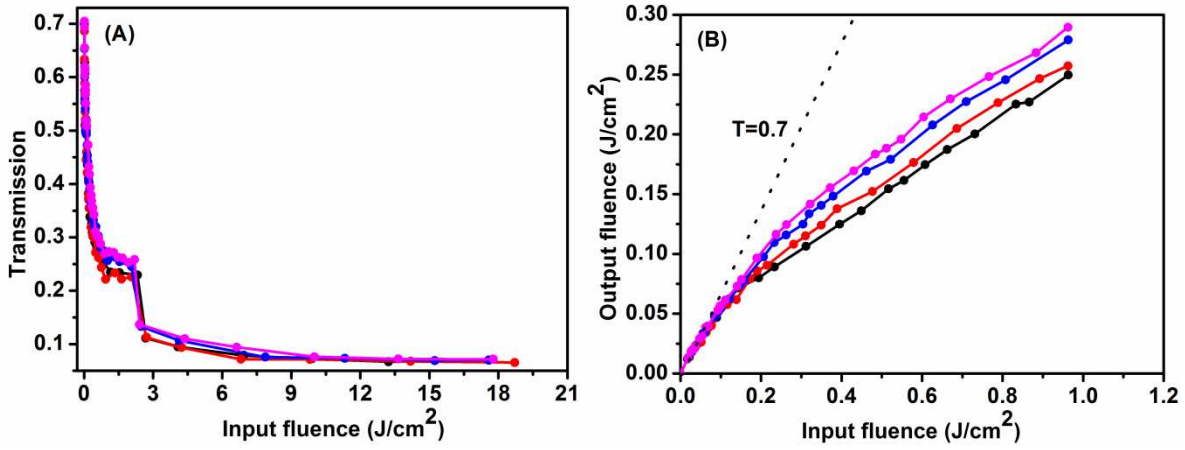


Fig. 5 Nonlinear transmission measurements (A) and optical limiting properties (B) of compounds **1** (black), **2** (red), **3** (blue) and $[H_2TPP][ClO_4]_2$ (pink) in DMF with the linear transmittance of 0.7 at 532 nm.

for compounds **1** - **3** and $[H_2TPP][ClO_4]_2$ when the input fluence is reached at 0.88 J/cm$^2$, and the transmission then remain nearly constant in the fluence range of 0.88 - 2.15 J/cm$^2$. Interestingly, the transmission shows a drastically decrease when the input fluence is up to 2.15 J/cm$^2$ and rapidly keep nearly constant again at *ca*. T = 7%. So far, sseveral mechanisms such as electron delocalization and thermal effect and so on have been reported to be responsible for the optical limiting activity of the materials. In our case, when input fluence is lower than 2.15 J/cm$^2$, the decrease and the following constant in transmission might be attributed to the nonlinear RSA and refraction arising from the π-conjugated electron delocalization of porphyrin.[46] When input fluence is greater than 2.15 J/cm$^2$, the drastically decrease in transmission imight be due to the contribution of thermal effect to the NLO properties.[47,48] It is clear from the above result that the porphyrin-POM supramolecular compounds can strongly attenuate intense, potentially dangerous optical beams, while exhibiting high transmittance for low-intensity ambient light, and are potential candidates in the field of OL.

Indeed, the solutions of the compounds in DMF (Fig 5B) show a typical transmittance profile of OL materials with a linear increase in output fluence followed by a decrease in the slope. For $[H_2TPP][ClO_4]_2$, the deviation from linearity occurs at 0.093 J/cm$^2$, whereas, for compounds **1** - **3** it occurs at 0.069, 0.075 and 0.085 J/cm$^2$, respectively. This demonstrates that compounds **1** - **3** show better limiting actions, which are superior to $[H_2TPP][ClO_4]_2$ in terms of onset of OL.[49] The OL thresholds, defined as the incident energy at which the transmittance is half of the initial linear transmittance,[50,51] are calculated (Table 1). From Table 1, it is known that the OL thresholds of compounds **1** - **3** show the following tend: compound **3** > compound **2** > compound **1**. The compound **1** shows a comparable performance (0.28 J/cm$^2$) with the most well-known OL material such as In(Pc*)Cl (0.27 J/cm$^2$, obtained under the same experimental conditions as for the compounds **1** - **3**),[52] indicating that the porphyrin-POM hybrids are potentially rich OL materials based on nonlinear RSA and refraction.

It is well-know that NLO property is related to the transition energy of the product. The smaller transition energy leads to a larger charge transfer.[53] Therefore, the larger charge transfer will come into being under the external electronic field and further leads to good nonlinear optical response. In our system, it is observed that the HOMO-LUMO gap $E_g$ (transition energy) values of compounds **1** - **3** (derived from the absorption edges of the spectra by equation $E_g = 1240/\lambda$ (λ is absorption edge, Fig. S5)[54]) increase in an order: $E_g$ (**1**) < $E_g$ (**2**) < $E_g$ (**3**), while the second hyperpolarizability $\gamma$ values and the OL performance decrease as follows: $\gamma$ (**1**) > $\gamma$ (**2**) > $\gamma$ (**3**). This observation matches well with the experimental results observed in our previous work[28] and other references.[53,55]

In order to get insight into the effect of POM anions on the third-order NLO and OL properties of the porphyrin-POM supramolecular compounds, the molecular orbitals levels of parent $[H_2TPP][ClO_4]_2$ and parent POMs were calculated by cyclic voltammetry (CV) spectra (Fig. S6).[54,56] It is evident from Fig. S6 that the introduction of V atom can increase the reduction potentials of the keggin type POM, however, the reduction potentials of these species do not vary monotonically with the number of vanadium atoms substituted. The mono-vanadium-substituted species $SWV_1$ exhibits the maximum reduction potential value (0.64 V) among the parent POMs, and $SWV_2$ has a slightly greater reduction potential (0.07 V) than SW (-0.53 V). Thus, the order of the reduction potentials for these substituted species is $SWV_1$ > $SWV_2$ > SW. It should be noted that quite similar observation was also found in the vanadium-substituted species $H_{n+3}PV_nM_{12-n}O_{40}$ (n = 0 – 3; M = Mo, W) where the reduction potentials of them are decreasing in the following order[57]: $H_4PVMo_{11}O_{40}$ (0.261 V) > $H_5PV_2Mo_{10}O_{40}$ (0.233 V) > $H_6PV_3Mo_9O_{40}$ (0.168 V) > $H_3PMo_{12}O_{40}$ (-0.082 V), $H_4PVW_{11}O_{40}$ (0.224 V) > $H_5PV_2W_{10}O_{40}$ (0.050 V) > $H_6PV_3W_9O_{40}$ (0.045 V) > $H_3PW_{12}O_{40}$ (-0.491 V).

Table 1 The third-order nonlinear parameters obtained by Z-scan measurements, HOMO-LUMO gaps $E_g$, LUMO energy levels, and $\Delta E$ ($[H_2TPP][ClO_4]_2$ - POM).

| Compounds | limiting threshold (J/cm$^2$) | $\beta \times 10^{-5}$ (esu) | $n_2 \times 10^{-10}$ (esu) | $\chi^{(3)} \times 10^{-11}$ (esu) | $\gamma \times 10^{-29}$ (esu) | $E_g$ (eV) | $E_{LUMO}$ (eV) | $\Delta E$ ($[H_2TPP][ClO_4]_2$ - POM)[a] |
|---|---|---|---|---|---|---|---|---|
| $[H_2TPP][ClO_4]_2$ | 0.63 | 1.31 | -1.74 | 3.35 | 5.78 | 1.88 | -3.46 | |
| compound **1** | 0.28 | 1.50 | -2.22 | 4.15 | 7.05 | 1.84 | | |
| $SWV_1$ | | | | | | | -4.89 | 1.43 |
| compound **2** | 0.37 | 1.46 | -2.09 | 3.94 | 6.59 | 1.86 | | |
| $SWV_2$ | | | | | | | -4.32 | 0.86 |
| compound **3** | 0.54 | 1.37 | -1.97 | 3.77 | 6.29 | 1.87 | | |
| SW | | | | | | | -3.73 | 0.37 |
| In(Pc*)Cl | 0.27[b] | | | | | | | |

[a]$\Delta E$ ($[TPP][ClO_4]_2$ -POM) = $E_{LUMO}$ ($[H_2TPP][ClO_4]_2$) - $E_{LUMO}$ (POM), [b]Cited from reference[52] which were measured under the same experimental conditions as for the compounds **1 - 3**.

Journal Name

RSCPublishing

ARTICLE

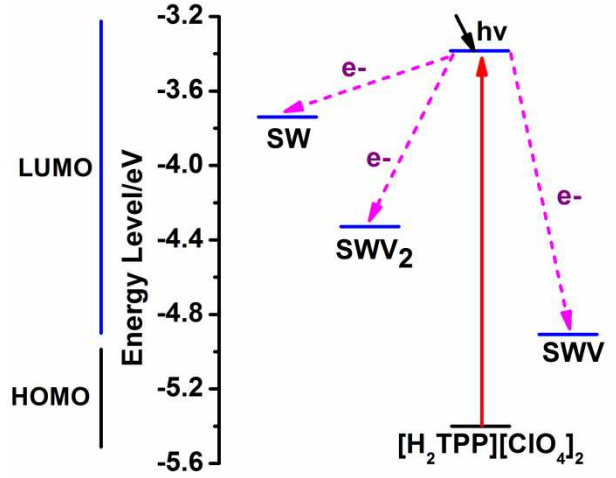


Fig. 6 Energy level and electron-transfer processes diagram of $[H_2TPP][ClO_4]_2$, POMs molecules. Color code: blue, LUMO level; black, HOMO level.

According to the known equations,[54,56] namely, $E_{LUMO}$ (eV) = -e (4.8 - $E_{FOC}$ + $E_{red}$) ($E_{red}$ is the onset of reduction potential of POMs, $E_{FOC} = (E_{ox} + E_{red})/2$ is energy level of ferrocene used as standard), and $E_{LUMO}$ (eV) = -e (4.8 - $E_{FOC}$ + $E_{ox}$) + $E_g$ ($E_{ox}$ is the onset of oxidation potential of $[H_2TPP][ClO_4]_2$, $E_{FOC} = (E_{ox} + E_{red})/2$ is energy level of ferrocene used as standard, $E_g$ is the HOMO-LUMO gap of $[H_2TPP][ClO_4]_2$), the LUMO levels of $[H_2TPP][ClO_4]_2$ and parent POMs are calculated and listed in Table 1. From the data in Table 1, it is obvious that the LUMO level of the POMs is found lower than that of $[H_2TPP][ClO_4]_2$, implying that excited electrons could inject from the porphyrin to the POMs[58,59] and make the resulting porphyrin-POM hybrids more activated when exposed in laser, which results in the enhancement of nonlinear response. Thus, the porphyrin-POM hybrids display higher third-order and OL response than the parent porphyrin. Meanwhile, it is observed that the discrepancy between LUMO levels of $[H_2TPP][ClO_4]_2$ and that of POMs, $\Delta E$ ($[H_2TPP][ClO_4]_2$ - POM) are decreasing in following order: $\Delta E$ ($[H_2TPP][ClO_4]_2$ – $SWV_1$) > $\Delta E$ ($[H_2TPP][ClO_4]_2$ - $SWV_2$) > $\Delta E$ ($[H_2TPP][ClO_4]_2$ - SW), while the $\gamma$ values and the OL performances are decreasing as follows: compound **1** > compound **2** > compound **3**. Thus, it can be deduced that the $\gamma$ values are directly proportional to $\Delta E$($[H_2TPP][ClO_4]_2$ - POM), while limiting thresh hold values are inversely proportional to $\Delta E$($[H_2TPP][ClO_4]_2$ - POM). In this context, low-lying LUMO levels of POMs, which can be further lowered by the introduction of V atom while not vary monotonically with the number of vanadium atoms substituted, are thought as the principle factor for the improved NLO and OL response in these porphyrin-POM systems.

## Conclusions

In conclusion, three new porphyrin-POM hybrids showing significant nonlinear reverse saturated absorption, self-defocusing behavior and excellent OL performance have been prepared and characterized. The vanadium-substitution in the Keggin-type POMs anion is found to be beneficial for the improvement of third-order NLO and OL properties of resulting porphyrin-POM hybrids while not vary monotonically with the number of vanadium atoms substituted. The facile charge transfer from excited porphyrin to POMs in the hybrids is thought to be responsible for the enhancement of these properties. The present work donates important insight into the NLO properties of porphyrin–POM hybrids, and could provide a new guide for the design of NLO materials with enhanced NLO properties based on porphyrin-polyoxometalate hybrids.

**Acknowledgements**

The financial support of the NSFC (Grant No. 20771012 and No. 21371020), PCSIRT (No. IRT1205) and Beijing Engineering Center for Hierarchical Catalysts is greatly acknowledged. Y. Zhou thanks Prof. Enbo Wang for his kind instruction and prompting and dedicates this paper on the occasion of his 80th birthday. Prof. Xue Duan of Beijing University of Chemical Technology is greatly acknowledged for his kind support.

## Notes and references

[a] State Key Laboratory of Chemical Resource Engineering, Institute of Science, Beijing University of Chemical Technology, Beijing 100029, P. R. China.

[b] Laboratory of Optical Physics, Institute of Physics, Chinese Academy of Sciences, Beijing 100190, P. R. China.

Electronic Supplementary Information (ESI) available: detailed IR spectra, UV spectra and CV spectra. DOI: 10.1039/b000000x/

*Corresponding author. Tel.: +86-10-64414640; e-mail: zhouys@mail.buct.edu.cn; ljzhang@mail.buct.edu.cn

1. L.M. Caroline, Ph.D. Thesis, Growth and Characterization of Some Organic and Semiorganic Amino Acid Based Nonlinear Optical Single Crystals, Bharath University, 2010.
2. D. M. Burland, R. D. Miller and C. A. Walsh, *Chem. Rev.*, 1994, **94**, 31.
3. G. I. Stegeman, D. J. Hagan and L. Torner, *Opt. Quant. Electron.*, 1996, **28**, 1691.
4. Q. D. Zheng, G. S. He and P. N. Prasad, *Chem. Phys. Lett.*, 2009, **475**, 250.
5. L. W. Tutt and A. Kost, *Nature*, 1992, **356**, 225.
6. T. Zhang, L. K. Yan, S. Cong, W. Guan and Z. M. Su, *Inorg. Chem. Front.*, 2014, **1**, 65.
7. D. Koszelewski, A. Nowak-Król, M. Drobizhev, C. J. Wilson,

J. E. Haley, T. M. Cooper, J. Romiszewski, E. Górecka, H. L. Anderson, A. Rebane and D. T. Gryko, *J. Mater. Chem. C,* 2013, **1**, 2044.
8. K. B. Manjunatha, R. Dileep, G. Umesh and B. R. Bhat, *Opt. Mater.*, 2013, **35**, 1366.
9. K. Traskovskis, K. Lazdovica, A. Tokmakovs, V. Kokars and M. Rutkis, *Dyes Pigm.,* 2013, **99**, 1044.
10. M. J. Cho, D. H. Choi, P. A. Sullivan, A. J. P. Akelaitis and L. R. Dalton, *Prog. Polym. Sci.*, 2008, **33**, 1013.
11. C. L. Lü and B. Yang, *J. Mater. Chem*., 2009, **19**, 2884.
12. C. Sanchez, B. Lebeau, F. Chapu and J. P. Boilot, *Adv. Mater*., 2003, **15**, 1969.
13. G. Brusatin and R. Signorini, *J. Mater. Chem.*, 2002, **12**, 1964.
14. W. H. Bi, N. Louvain, N. Mercier, J. Luc, I. Rau, F. Kajzar and B. Sahraoui, *Adv. Mater*., 2008, **20**, 1013.
15. M. O. Senge, M. Fazekas, E. G. A. Notaras, W. J. Blau, M. Zawadzka, O. B. Locos and E. M. N. Mhuircheartaigh, *Adv. Mater*., 2007, **19**, 2737.
16. M. Calvete, G. Y. Yang and M. Hanack, *Synt. Met.*, 2004, **141**, 231.
17. Z. B. Liu, Z. Guo, X. L. Zhang, J. Y. Zheng and J. G. Tian, *Carbon*, 2013, **51**, 419.
18. Z. B. Liu, J. G. Tian, Z. Guo, D. M. Ren, F. Du, J. Y. Zheng and Y. S. Chem, *Adv. Mater.*, 2008, **20**, 511.
19. A. J. Wang, L. L. Long, W. Zhao, Y. L. Song, M. G. Humphrey, M. P. Cifuentes, X. Z. Wu, Y. S. Fu, D. D. Zhang, X. F. Li and C. Zhang, *Carbon*, 2013, **53**, 327.
20. X. J. Liu, J. K. Feng, A. M. Ren and X. Zhou, *J. Mol. Struct*., 2003, **635**, 191.
21. R. Misra, R. Kumar, V. PrabhuRaja and T. K. Chandrashekar, *J. Photochem. Photobiol. A*, 2005, **175**, 108.
22. C. Hill, *Chem. Rev*., 1998, **98**, 1.
23. D. L. Long, E. Burkholder and L. Cronin, *Chem. Soc. Rev*., 2007, **36**, 105.
24. T. Yamase, *Chem. Rev*., 1998, **98**, 307.
25. C. Yao, L. K. Yan, W. Guan, C. G. Liu, P. Song and Z. M. Su, *Dalton Trans*., 2010, **39**, 7645.
26. T. Zhang, N. N. Ma, L. K. Yan, S. Z. Wen, T. Y. Ma and Z. M. Su, *J. Mol. Graphics Modell*., 2013, **46**, 59.
27. C. Yao, B. Hu, Q. W. Wang, P. Song and Z. M. Su, *Russ. J. Phys. Chem. A*, 2014, **88**, 970.
28. Z. H. Shi, Y. S. Zhou, L. J. Zhang, S. Hassan and N. N. Qu, *J. Phys. Chem. C*, 2014, **118**, 6413.
29. Y. S. Zhou, E. B. Wang, J. Peng, J. Liu, C. W. Hu, R. D. Huang and X. Z. You, *Polyhedron*, 1999, **18**, 1419.
30. L. J. Zhang, Y. S. Zhou and R. X. Han, *Eur. J. Inorg. Chem.,* 2010, **17**, 2471.
31. L. J. Zhang, Z. H. Shi, L. H. Zhang, Y. S. Zhou and S. Hassan, *Mater. Lett.,* 2012, **86**, 62.
32. Y. S. Zhou, Z. H. Shi, L. J. Zhang, S. Hassan and N. N. Qu, *Appl. Phys. A.,* 2013, **113**, 563.
33. Y. S. Zhou, X. Wang and L. J. Zhang, *CN Pat*., 200810224493.1, 2008.
34. Y. S. Zhou, W. X. Tang, L. J. Zhang and Y. H. Li, *CN Pat*., 201010140796.2, 2010.
35. Y. S. Zhou, R. X. Han, L. J. Zhang, Y. H. Li and L. H. Zhang, *Chem. J. Chinese Universities,* 2008, **29**, 1299.
36. Y. S. Zhou, Z. H. Shi and L. J. Zhang, *CN Pat*., 2001210046706.2, 2012.
37. A. D. Adler, F. R. Longo and J. D. Finarlli, *Inorg. Chem.*, 1966, **32**, 476.
38. H. Sadayuki, T. Masayo, H. Mitsuru, H. Ayumi and H. Masato, *Bull. Chem. Soc. Jpn.*, 2004, **77**, 519.
39. M. Meot-Ner and A. D. Adler, *J. Am. Chem. Soc.,* 1975, **97**, 5107.
40. J. Y. Niu, X. Z. You, C. Y. Duan, H. K. Fun and Z. Y. Zhou, *Inorg. Chem.*, 1996, **35**, 4211.
41. M. Kamachi, X. S. Cheng, T. Kida, A. Kajiwara, M. Shibasaka, and S. Nagataf, *Macromolecules,* 1987, **20**, 2665.
42. Z. D. Hill and P. Maccarthyl, *J. Chem. Educ.*, 1986, **63**, 162.
43. T. Norman, Conference on Laser and Electro-Optics, OSA Technical Digest Series, Washington DC, 1993.
44. M. Sheik-Bahae, A. A. Said, T. H. Wei, D. J. Hagan and E. W. Van Stryland, *IEEE J. Quant. Electron.,* 1990, **26**, 760.
45. S. F. Wang, W. T. Huang, T. Q. Zhang, Y. Hong, Q. H. Gong, Y. Okuma, M. Horikiri and Y. F. Miura, *Appl. Phys. Lett.*, 1999, **75**, 1845.
46. Z. B. Liu, Y. Z. Zhu, Y. Zhu, S. Q. Chen, J. Y. Zheng, and J. G. Tian, *J. Phys. Chem. B*, 2006, **110**, 15140.
47. L. Polavarapu, N. Venkatram, W. Ji, and Q. H. Xu, *ACS Appl. Mater. Interfaces*, 1999, **10**, 2298.
48. H. G. Yaglıoglu, M. Arslan, S. Abdurrahmanoglu, H. Ünver, A. Elmali and Ö. Bekaroglu, *J. Phys. Chem. Solids*, 2008, **69**, 161.
49. P. Gautam, B. Dhokale, V. Shukla, C. P. Singh, K. S. Bindra and R. Misra, *J. Photochem. Photobiol. A*, 2012, **239**, 24.
50. Y. Li, T. M. Pritchett, J. Huang, M. Ke, P. Shao and W. Sun, *J. Phys. Chem. A*, 2008, **112**, 7200.
51. Y. Chen, M. Hanack, Y. Arakic and O. Ito, *Chem. Soc. Rev*., 2005, **34**, 517.
52. H. L. Wang, D. D. Qi, Z. Xie, W. Cao, K. Wang, H. Shang and J. Z. Jiang, *Chem. Commun*., 2013**, 49**, 889.
53. G. C. Yang, W. Guan, L. K. Yan and Z. M. Su, *J. Phys. Chem. B*, 2006, **110**, 23092.
54. X. B. Sun, Y. Q. Liu, S. Y. Chen, W. F. Qiu, Y. Gui, Y. Q. Ma, T. Qi, H. J. Zhang, X. J. Xu and D. B. Zhu, *Adv. Funct. Mater.,* 2006, **16**, 917.
55. M. G. Victor, L. Christoph and B. Jean-Luc, *J. Am. Chem. Soc*., 2003, **125**, 15651.
56. B. R. Hyun, Y. W. Zhong, A. C. Bartnik, L. F. Sun, H. D. Abrun, F. W. Wise, J. D. Goodreau, J. R. Matthews, T. M. Leslie and N. F. Borrelli, *ACS Nano*, 2008, **2**, 2206.
57. I. K. Song and M. A. Barteau, *J. Mol. Catal. A*: *Chem*. 2004, **212**, 229.
58. Y. B. Yang, L. Xu, F. Y. Li, X. G. Du and Z. X. Sun, *J. Mater. Chem*., 2010, **20**, 10835.
59. S. Bhattacharyya, E. Kymakis, and G. A. J. Amaratunga, *Chem. Mater*., 2004, **16**, 4819.



 